Crystalline Sponge Method

Deutsche Ausgabe: DOI: 10.1002/ange.201509801
Internationale Ausgabe: DOI: 10.1002/anie.201509801

In Situ Observation of Thiol Michael Addition to a Reversible Covalent Drug in a Crystalline Sponge

Vincent Duplan, Manabu Hoshino, Wei Li, Tadashi Honda, and Makoto Fujita**

Dedicated to Professor Iwao Ojima on the occasion of his 70th birthday

Abstract: *A reversible Michael addition reaction between thiol nucleophiles and cyanoenones has been previously postulated to be the mechanism-of-action of a new family of reversible covalent drugs. However, the hypothetical Michael adducts in this mechanism have only been detected by spectroscopic methods in solution. Herein, the crystallographic observation of reversible Michael addition with a potent cyanoenone drug candidate by means of the crystalline-sponge method is reported. After inclusion of the cyanoenone substrate, the sponge crystal was treated with a thiol solution. Subsequent crystallographic analysis confirmed the single-crystal-to-single-crystal transformation of the substrate into the impermanent Michael adduct.*

The Michael addition reaction of thiols with α-cyano-α,β-unsaturated carbonyl compounds is known to rapidly and reversibly proceed at physiological pH.[1] This reaction has been postulated to be the mechanism-of-action for a new family of bioactive molecules containing non-enolizable cyanoenones.[2] These molecules demonstrate unique biological features by selectively targeting protein cysteine residues in a reversible covalent fashion,[3] avoiding off-target drug interactions. Owing to the reversible nature of the reaction, toxicity issues commonly associated with covalent protein modifications can be minimized. One compound from this family, bardoxolone methyl (CDDO-Me; **1**), is currently in a phase II clinical trial,[4] and some candidates such as MCE-23 (**2**), which have different features from those of **1**, are being developed.[2,5] These molecules are potent activators of the Keap1/Nrf2/ARE pathway,[6] which leads to the suppression of inflammation and cancer.[7]

Although the reversible Michael adducts involved in equilibrium mixtures have been detected in solution by NMR, UV/Vis absorption spectroscopy, and mass spectrometry, they have never been isolated and structurally characterized because of the rapid equilibrium that favors the reverse reaction.[2,5] Quite recently, a domain of Keap1 was co-crystallized with CDDO and the crystal structure of the complex was solved. However, the low resolution data at 2.66 Å cannot confirm the cysteine Michael adduct structure.[8] The direct observation and characterization of these adducts at atomic resolution is thus particularly important to better understand the postulated mechanism-of-action for such reversible covalent drugs. Herein, we report the direct structural determination of this impermanent intermediate using the crystalline sponge method.[9–11] Crystalline sponges are porous coordination networks that absorb and orient guest molecules into their pores to make the guests detectable by X-ray crystallography. In this study, this method is applied for the first time using network **3** for the in situ crystallographic observation of a chemical reaction. We show that the Michael adduct intermediate generated in situ in the pores was trapped and crystallographically observed at an atomic resolution in the crystalline sponge.

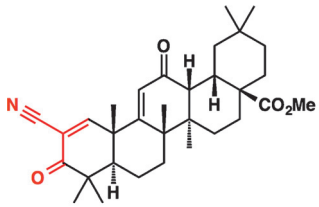

bardoxolone methyl (**1**)

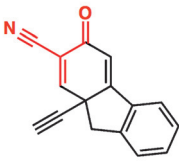

MCE-23 (**2**)

In this work, $\{[(ZnI_2)_3(tpt)_2]\cdot x\,(cyclohexane)\}_n$ (**3**; tpt = tris(4-pyridyl)-1,3,5-triazine) was used as the crystalline sponge.[12] This structure can strongly bind most small organic molecules because of the presence of many binding sites with different interaction modes: at the highly electron-deficient triazine core, charge-transfer, CH–π, and π–π interactions can occur, whereas hydrogen bonding between the pyridyl protons (donor sites) and iodine atoms (acceptor sites) is also possible, as revealed by many previous examples. In this study, MCE-23 (**2**) was selected as the target. This compound exhibits a highly electrophilic carbon–carbon double bond which is doubly conjugated to cyano and carbonyl groups. Consequently, the cyanoenone moiety is highly susceptible to nucleophilic attack by thiol reagents to form reversible covalent bonds (Scheme 1).

The structure of parent guest compound **2** was analyzed using the crystalline sponge method. A one-crystal-scale guest inclusion was examined under several different sets of conditions. Typically, a rod-shaped sponge crystal of **3**

[*] Dr. V. Duplan, Dr. M. Hoshino, Prof. Dr. M. Fujita
Department of Applied Chemistry
School of Engineering, The University of Tokyo
7-3-1 Hongo, Bunkyo-ku, Tokyo 113–8656 (Japan)
E-mail: mfujita@appchem.t.u-tokyo.ac.jp
Dr. W. Li, Prof. Dr. T. Honda
Institute of Chemical Biology and Drug Discovery
Stony Brook University
Stony Brook, NY 11794 (USA)

Supporting information for this article can be found under http://dx.doi.org/10.1002/anie.201509801.

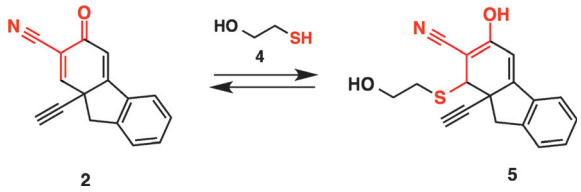

Scheme 1. The reversible Michael addition reaction of compound **2** to form compound **5** studied in this work.

(length ≈ 200 μm) was dipped in cyclohexane (80 μL) in a small glass vial. A solution of racemic **2** in CH_2Cl_2 (1 μg μL^{-1}; 5 μL:5 μg) was added to the vial. The vial was capped and a needle was inserted to allow slow evaporation of the solvent. The vial was then placed in an incubator at 50 °C for 2 days. In most cases, the examined crystals had cracked, presumably because of the occurrence of host–guest interactions which were too strong, but fortunately some were tolerant to these interactions. After preliminary measurement with an X-ray scanner, data for the crystal with the best diffraction properties was collected using an in-house X-ray diffractometer (Cu Kα radiation).

The crystallographic analysis of the collected data clearly shows two crystallographically independent molecules of **2** with the same stereochemical configuration at two distinct sites *a* and *b* (Figure 1; sites *a* and *b* are indicated in Figure 2a). Two other molecules of **2** with the opposite configuration are evident at the *a*′ and *b*′ sites, which are symmetrically inverted sites that are crystallographically equivalent to the *a* and *b* sites, respectively. At site *a*, **2** is stabilized inside the pore by hydrogen bonding between the carbonyl group and two C–H bonds from electron-deficient pyridine moieties. Additional CH–π interactions are found between the phenyl ring and the pyridyl C–H bonds. At site *b*, the benzene ring strongly interacts with the tpt ligand through π–π stacking. As all the guest molecules observed at the *a*, *b*, *a*′, and *b*′ sites lie on a twofold axis, the guest population is estimated to be 25% for each. In other words, a racemic mixture of cyanoenone **2** was trapped inside the pores with an overall occupancy of 100%.[13,14] Figure 1 shows the configuration of guest molecule **2** at site *a* in the crystalline sponge.

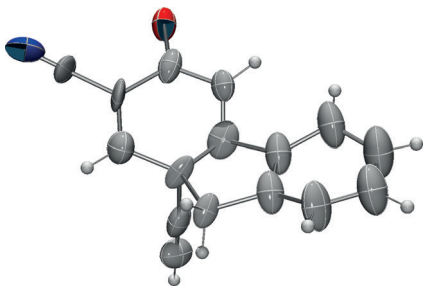

Figure 1. ORTEP diagram of cyanoenone **2** as observed in the inclusion complex **2**·**3** before the reaction with the thiol reagent. Thermal ellipsoids are set at 50% probability. For guest **2**, two crystallographically independent molecules were observed at sites *a* and *b* in the pores of the crystalline sponge. Only the guest **2** at site *a* is shown here (see the Supporting Information). Atom colors: N = blue; O = red; C = gray; H = white.

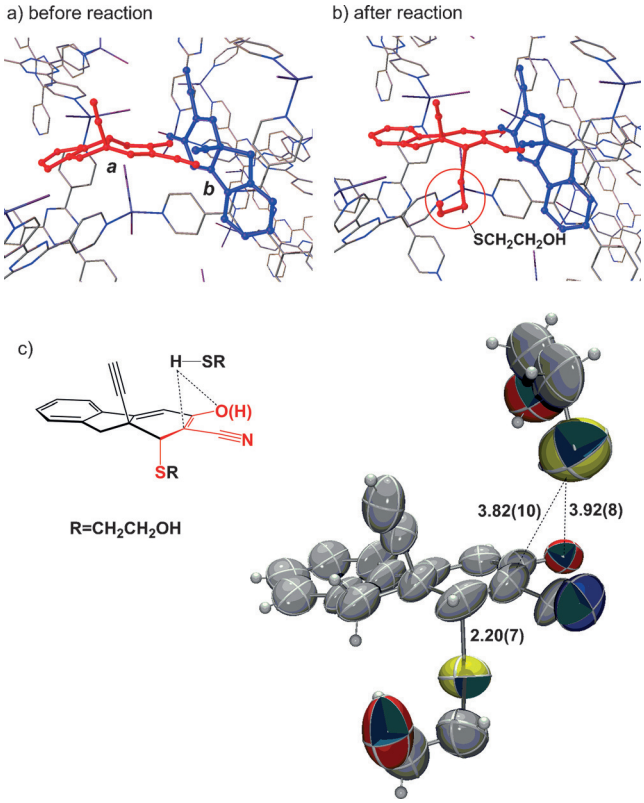

Figure 2. Crystal structures of the guests trapped in the pore of the sponge a) before and b) after the thiol addition. Guest molecules at site *a* are shown completely in red and at site *b* in blue. c) ORTEP diagram (thermal ellipsoids set at 50% probability) of Michael adduct **5** observed in inclusion complex **5**·**3** after the reaction. One free molecule of **4** is observed near the enol part of adduct **5** at a distance close enough for interactions to occur.

The detailed structure analysis is described in the Supporting Information.

We then examined the reversible Michael addition of a thiol reagent with cyanoenone **2** trapped inside crystalline sponge **3**. By applying many different conditions (such as, reaction time, temperature, thiol reagent, and co-solvent), we were able to find appropriate soaking conditions (2 μg of 2-mercaptoethanol (**4**), 4 °C for 5 days) to observe the formation of the expected Michael adduct **5** inside the pore. Even under the same conditions, however, the crystals were often cracked and the data quality depended on subtle differences in the sponge crystal character (such as size, shape, and habit). To further optimize the soaking conditions, high throughput screening for the Michael addition process was examined. The inclusion of **2** in sponge **3** was thus reproduced with 65 different sponge crystals. After guest inclusion, all of the crystals were transferred to small glass vials and, for each crystal, 20 μL of cyclohexane and 2 μg of 2-mercaptoethanol (**4**; 2 μL of a 1 μg μL^{-1} solution in CH_2Cl_2) were added. The vials were then capped with a screw cap with the lid pierced by a needle and kept at 4 °C for 5 days. Shortly afterwards, the 65 sets of crystals were tested for their X-ray diffraction qualities with an X-ray scanner for high-throughput screening.

Among the 65 crystals, the best sponge crystal ($260 \times 130 \times 60\ \mu m^3$) that diffracted sharply with non-split spots and suitable intensity for data collection was identified. The diffraction pattern of the corresponding crystal is presented in Figure S2 in the Supporting Information. The selected crystal was mounted and measured on an in-house X-ray diffractometer (Cu Kα radiation) at 100 K.

We were delighted to detect the thiol Michael adduct **5** formed in situ at site *a* of the pore (Figure 2b). Interestingly, the Michael addition was not detected at site *b* and the starting cyanoenone **2** remained unchanged at this site. This is presumably because of the efficient stacking of **2** on the tpt ligand at site *b*, which prevents the nucleophilic attack of the thiol on **2** (Figure 2a). In contrast, cyanoenone **2** at site *a* is not stacked with the tpt ligand and some free space exists around the reaction site before the reaction; this allows the nucleophilic addition of thiol **4** to occur. In the reversible Michael adduct **5** found at site *a* (Figure 2c), the nitrile group and C–O bond on the cyanoenone ring are coplanar ($\varnothing_{O\text{-}C\text{-}C\text{-}CN} = 12(8)°$). Thus, it is strongly suggested that the adduct adopts an enol form rather than a keto form.

The enol form of the adduct is consistent with the previous spectroscopic observation of reversible Michael adducts in solution with similar compounds.[2,3] Corresponding to these results, a decrease of the intensity of the C=O absorption band was detected for the crystal in which the in situ Michael addition reaction had occurred. Before and after the thiol addition, single crystal FTIR measurements were carried out to obtain further support for the occurrence of in situ Michael addition. As shown in Figure 3, we detected a decrease of about 40% in the intensity of the C=O stretching vibrational band at 1660 cm^{-1} (see the Supporting Information). The relative intensities of the other bands remained almost the same. These additional analyses were essential not only to confirm the formation of the reversible Michael adduct but also to interpret the observed X-ray data more reliably.

It is noteworthy that the equilibrium of the reversible Michael addition was almost exclusively pushed towards the formation of the adduct at site *a* in the crystal; this is in sharp contrast to the solution-state equilibrium at low concentrations, which favors the starting enones. Presumably, excess thiol **4** is absorbed into the confined cavity of the crystalline sponge with a high local concentration, pushing the equilibrium toward the Michael adduct. In fact, the crystallographic analysis revealed the co-existence of excess **4** at a location close to the adduct in the pore. The excess thiol was extracted from the crystal and was confirmed to have existed in the pore using qualitative NMR analysis.

We noticed that the newly formed C–S bond (2.20(7) Å; Figure 2c) was slightly elongated (compared to the typical length of 1.87 Å[15]) and that one free thiol molecule (**4**) was in close proximity to the enolate oxygen atom ($S\cdots O_{C=COH} = 3.92(8)$ Å). The sulfur atom of **4** is also close to the enolate carbon center ($S\cdots C_{C<C=>COH} = 3.82(10)$ Å). These observations imply a concerted, push–pull mechanism for this Michael addition in which two thiols are involved: one as a nucleophile and another as a Brønsted acid to activate the acceptor oxygen (Scheme 2). More specifically, these observations could be interpreted as indicative of a protonated

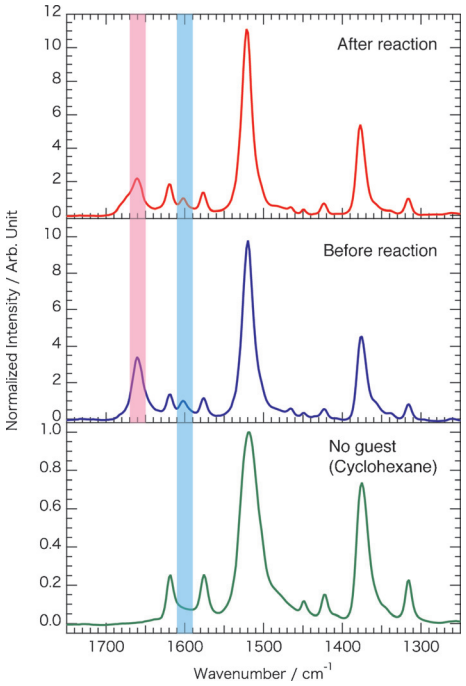

Figure 3. Single-crystal microscopic FTIR spectra of **5·3** (top), **2·3** (middle), and **3** (bottom). The spectra of **2·3** and **5·3** were normalized to the intensity of the absorption at 1600 cm^{-1} of the guest molecule (light blue strip). Comparison of the spectra before and after the reaction shows that the intensity of the C=O stretching vibrational band at 1660 cm^{-1} decreased by about 40% (pink strip).

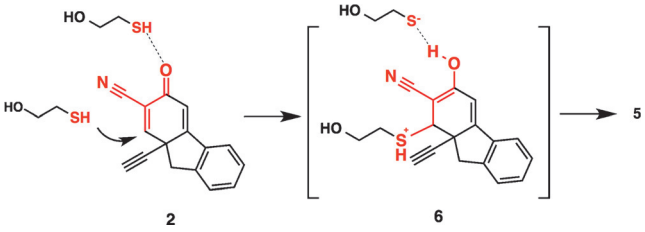

Scheme 2. A plausible push–pull mechanism for the Michael addition in crystalline sponge **3**. The association of the two thiol moieties was indicated by the X-ray crystallographic analysis (see Figure 2).

reaction intermediate **6** before reaching deprotonated product **5** or, more reasonably, an averaged structure of **2**, **5**, and/or **6**. The slight elongation of the C–S bond explains well the reversible nature of this Michael addition and is in good agreement with the postulated mechanism-of-action for the cyanoenone-type reversible covalent drugs.

Another important feature of our results is that the Michael addition reaction took place in a stereoselective fashion and only one diastereomer of the Michael adduct was detected. The stereoselectivity of the reaction may be explained by the directing effect of the adjacent alkyne group.

To summarize, the crystalline sponge method was successfully used to visualize an impermanent intermediate in the reversible Michael addition of a thiol to the non-enolizable cyanoenone acceptor **2**, a potent activator of the Keap1/Nrf2/ARE pathway. The in situ crystallographic observation of the

adduct provides strong support for the postulated, yet quite unusual, mechanism-of-action of this reversible covalent drug, which has attracted a great deal of interest among the scientific community.[16–18] Particularly, 3D structure determination of the unstable Michael adduct encourages researchers to explore reversible covalent drugs containing a fragment with a non-enolizable α-cyano-α, β-unsaturated carbonyl functionality. More generally, our results show that the crystalline sponge method can support medicinal and chemical biology studies by the visualization of expected biochemical transformations that are difficult to detect by means of conventional spectroscopic analysis or under common chemical conditions.

Furthermore, the present research expands the potential ability of the crystalline sponge to act as a molecular flask in which pseudo-solution-state reactions are performed and with which snapshots of the reaction can be obtained by X-ray crystallography. The pre-installment of reaction sites on the host framework, which was necessary in previous examples of X-ray reaction tracing in porous complexes,[19,20] is unnecessary in the present study. The chemical reaction can be performed simply by treating the crystalline sponge first with a substrate followed by a reagent of interest.

Experimental Section

The preparation of crystals **2·3** and **5·3** is described in the text. Spectroscopic and X-ray experiments are described in detail in the Supporting Information.

Crystallographic data of **2·3**: Refined formula = $C_{63.55}H_{67.60}N_{12.50}O_{0.50}Zn_3I_6$, formula weight ($M_r$) = 1972.01, monoclinic crystal system, space group = $C2/c$, $Z = 8$. 15856 unique reflections merged from 57472 recorded ones ($3.681° < \theta < 74.360°$) were used for structural analysis ($R_{int} = 0.0361$). Lattice parameters, R-factor on $F^2 > 2\sigma(F^2)$, and weighted R-factor are as follows: $a = 34.9634(12)$, $b = 14.8809(3)$, $c = 31.2738(10)$ Å; $\beta = 103.892(3)°$; $V = 15795.4(8)$ Å^3; $R = 0.0621$, $wR = 0.2199$, $S = 1.037$. Calculated density is 1.659. Linear absorption coefficient (μ) is 19.810. Residual electron density (max/min) is 0.764/−1.269 e Å^{-3}.

Crystallographic data **5·3**: Refined formula = $C_{58.50}H_{58.50}N_{12.50}OS_{0.50}Zn_3I_6$, formula weight ($M_r$) = 1926.21, monoclinic crystal system, space group = $C2/c$, $Z = 8$. 15949 unique reflections merged from 57847 recorded ones ($3.660° < \theta < 74.654°$) were used for structural analysis ($R_{int} = 0.0448$). Lattice parameters, R-factor on $F^2 > 2\sigma(F^2)$, and weighted R-factor are as follows: $a = 34.8709(19)$ Å, $b = 14.9376(4)$ Å, $c = 31.235(2)$ Å; $\beta = 102.912(6)°$; $V = 15858.3(15)$ Å^3; $R = 0.0783$, $wR = 0.2288$, $S = 1.045$. Calculated density is 1.614. Linear absorption coefficient (μ) is 19.842. Residual electron density (max/min) is 0.748/−0.710 e Å^{-3}.

CCDC 1431774 (**2·3**) and 1431775 (**5·3**) contain the supplementary crystallographic data for this paper. These data are provided free of charge by The Cambridge Crystallographic Data Centre.

Acknowledgements

V.D. thanks JSPS for a Postdoctoral Fellowship for North American and European Researchers. T.H. thanks the Stony Brook Foundation and Reata Pharmaceuticals for financial support. W.L. thanks ICB&DD for Postdoctoral Scholarships. This research was carried out as a part of the JST-*ACCEL* project in which M.F. is a principle investigator.

Keywords: chemical equilibrium · crystalline sponge · Michael addition · reversible covalent inhibitors · structure elucidation

How to cite: *Angew. Chem. Int. Ed.* **2016**, *55*, 4919–4923
Angew. Chem. **2016**, *128*, 5003–5007

[1] a) R. B. Pritchard, C. E. Lough, D. J. Currie, H. L. Holmes, *Can. J. Chem.* **1968**, *46*, 775–781; b) I. M. Serafimova, M. A. Pufall, S. Krishnan, K. Duda, M. S. Cohen, R. L. Maglathlin, J. M. McFarland, R. M. Miller, M. Frödin, J. Taunton, *Nat. Chem. Biol.* **2012**, *8*, 471–476; c) Y. Zhong, Y. Xu, E. V. Anslyn, *Eur. J. Org. Chem.* **2013**, 5017–5021.

[2] a) R. D. Couch, R. G. Browning, T. Honda, G. W. Gribble, D. L. Wright, M. B. Sporn, A. C. Anderson, *Bioorg. Med. Chem. Lett.* **2005**, *15*, 2215–2219; b) T. Honda, H. Yoshizawa, C. Sundararajan, E. David, M. J. Lajoie, F. G. Favaloro, Jr., T. Janosik, X. Su, Y. Honda, B. D. Roebuck, W. G. Gordon, *J. Med. Chem.* **2011**, *54*, 1762–1778; c) S. Zheng, Y. R. S. Laxmi, E. David, A. T. Dinkova-Kostova, H. Shiavoni, Y. Ren, Y. Zheng, I. Trevino, R. Bumeister, I. Ojima, W. C. Wigley, J. B. Bliska, D. F. Mierke, T. Honda, *J. Med. Chem.* **2012**, *55*, 4837–4846.

[3] a) A. T. Dinkova-Kostova, K. T. Liby, K. K. Stephenson, D. W. Holtzclaw, X. Gao, N. Suh, C. Williams, R. Risingsong, T. Honda, G. W. Gribble, B. Sporn, P. Talalay, *Proc. Natl. Acad. Sci. USA* **2005**, *102*, 4584–4589; b) A. T. Dinkova-Kostova, P. Talalay, J. Sharkey, Y. Zhang, W. D. Holtzclaw, X. J. Wang, E. David, K. H. Schiavoni, S. Finlayson, D. F. Mierke, T. Honda, *J. Biol. Chem.* **2010**, *285*, 33747–33755.

[4] NCT02036970 study, Bardoxolone Methyl Evaluation in Patients With Pulmonary Hypertension (PH), ClinicalTrials.gov.

[5] W. Li, S. Zheng, M. Higgins, R. P. Morra, Jr., A. Mendis, C.-W. Chien, I. Ojima, D. F. Mierke, A. T. Dinkova-Kostova, T. Honda, *J. Med. Chem.* **2015**, *58*, 4738–4748.

[6] a) T. Dinkova-Kostova, W. D. Holtzclaw, R. N. Cole, K. Itoh, N. Wakabayashi, Y. Katoh, M. Yamamoto, P. Talalay, *Proc. Natl. Acad. Sci. USA* **2002**, *99*, 11908–19913; b) M. Kobayashi, L. Li, N. Iwamoto, Y. Nakajima-Takagi, H. Kaneko, Y. Nakayama, M. Eguchi, Y. Wada, Y. Kumagai, M. Yamamoto, *Mol. Cell. Biol.* **2009**, *29*, 493–502; c) J. D. Hayes, A. T. Dinkova-Kostova, *Trends Biochem. Sci.* **2014**, *39*, 199–218.

[7] a) E. R. Stadtman, B. S. Berlett, *Chem. Res. Toxicol.* **1997**, *10*, 485–494; b) L. M. Coussens, Z. Werb, *Nature* **2002**, *420*, 860–867.

[8] A. Cleasby, J. Yon, P. J. Day, C. Richardson, I. J. Tickle, P. A. Williams, J. F. Callahan, R. Carr, N. Concha, J. K. Kerns, H. Qi, T. Sweitzer, P. Ward, T. G. Davies, *PLoS One* **2014**, *9*, e98896.

[9] Y. Inokuma, S. Yoshioka, J. Ariyoshi, T. Arai, Y. Hitora, K. Takada, S. Matsunaga, K. Rissanen, M. Fujita, *Nature* **2013**, *495*, 461–466; Corrigendum: Y. Inokuma, S. Yoshioka, J. Ariyoshi, T. Arai, Y. Hitora, K. Takada, S. Matsunaga, K. Rissanen, M. Fujita, *Nature* **2013**, *501*, 262–262.

[10] For practical guidelines, see: a) Y. Inokuma, S. Yoshioka, J. Ariyoshi, T. Arai, M. Fujita, *Nat. Protoc.* **2014**, *9*, 246–252; b) M. Hoshino, A. Khutia, H. Xing, Y. Inokuma, M. Fujita, *IUCrJ.* **2016**, *3*, 139–151; c) T. R. Ramadhar, S.-L. Zheng, Y.-S. Chen, J. Clardy, *Acta Crystallogr. Sect. A* **2015**, *71*, 46–58.

[11] For applications in organic chemistry, see: a) D. Kamimura, D. Urabe, M. Nagatomo, M. Inoue, *Org. Lett.* **2013**, *15*, 5122–5125; b) E. V. Vinogradova, P. Müller, S. L. Buchwald, *Angew. Chem. Int. Ed.* **2014**, *53*, 3125–3128; *Angew. Chem.* **2014**, *126*, 3189–3192; c) A. G. O'Brien, A. Maruyama, Y. Inokuma, M. Fujita, P. S. Baran, D. G. Blackmond, *Angew. Chem. Int. Ed.* **2014**, *53*, 11868–11871; *Angew. Chem.* **2014**, *126*, 12062–12065; d) T. R. Ramadhar, S.-L. Zheng, Y.-S. Chen, J. Clardy, *Chem. Commun.* **2015**, *51*, 11252–11255; e) N. Zigon, M. Hoshino, S. Yoshioka, Y. Inokuma, M. Fujita, *Angew. Chem. Int. Ed.* **2015**, *54*, 9033–9037;

Angew. Chem. **2015**, *127*, 9161 – 9165; f) S. Yoshioka, Y. Inokuma, M. Hoshino, T. Sato, M. Fujita, *Chem. Sci.* **2015**, *6*, 3765 – 3768; g) S. Takizawa, K. Kishi, Y. Yoshida, S. Mader, F. Arteaga, S. Lee, M. Hoshino, M. Rueping, M. Fujita, H. Sasai, *Angew. Chem. Int. Ed.* **2015**, *54*, 15511 – 15515; *Angew. Chem.* **2015**, *127*, 15731 – 15735; h) S. Urban, R. Brkljača, M. Hoshino, S. Lee, M. Fujita, *Angew. Chem. Int. Ed.* **2016**, *55*, 2678 – 2682; *Angew. Chem.* **2016**, *128*, 2728 – 2732.

[12] a) K. Biradha, M. Fujita, *Angew. Chem. Int. Ed.* **2002**, *41*, 3392 – 3395; *Angew. Chem.* **2002**, *114*, 3542 – 3545; b) O. Ohmori, M. Kawano, M. Fujita, *J. Am. Chem. Soc.* **2004**, *126*, 16292 – 16295.

[13] G. M. Sheldrick, *Acta Crystallogr. Sect. A* **2008**, *71*, 3 – 8 (SHELXT).

[14] G. M. Sheldrick, *Acta Crystallogr. Sect. C* **2008**, *64*, 3 – 8 (SHELXL).

[15] CCDC (Mogul analysis details).

[16] A. J. Wilson, J. K. Kerns, J. F. Callahan, J. M. Christopher, *J. Med. Chem.* **2013**, *56*, 7463 – 7476.

[17] S. Krishnan, R. M. Miller, B. Tian, R. D. Mullins, M. P. Jacobson, J. Taunton, *J. Am. Chem. Soc.* **2014**, *136*, 12624 – 12630.

[18] P. A. Schwartz, P. Kuzmic, J. Solowiej, S. Bergqvist, B. Bolanos, C. Almaden, A. Nagata, K. Ryan, J. Feng, D. Dalvie, J. C. Kath, M. Xu, R. Wani, B. W. Murray, *Proc. Natl. Acad. Sci. USA* **2014**, *111*, 173 – 178.

[19] a) T. Kawamichi, T. Haneda, M. Kawano, M. Fujita, *Nature* **2009**, *461*, 633 – 635; b) Y. Inokuma, M. Kawano, M. Fujita, *Nat. Chem.* **2011**, *3*, 349 – 358; c) K. Ikemoto, Y. Inokuma, K. Rissanen, M. Fujita, *J. Am. Chem. Soc.* **2014**, *136*, 6892 – 6895.

[20] R. Kubota, S. Tashiro, M. Shiro, M. Shionoya, *Nat. Chem.* **2014**, *6*, 913 – 918.

Received: October 19, 2015
Revised: January 24, 2016
Published online: March 11, 2016

